

# Amplitude-Based Sequential Optimization of Energy Harvesting with Reconfigurable Intelligent Surfaces

Morteza Tavana\*, Meysam Masoudi<sup>†</sup>, and Emil Björnson\*

\*School of Electrical Engineering and Computer Science, KTH Royal Institute of Technology, Stockholm, Sweden

<sup>†</sup>Ericsson, Global AI Accelerator (GAIA) unit, Sweden

E-mail: \*{morteza2, emilboj}@kth.se, <sup>†</sup>meysam.masoudi@ericsson.com

**Abstract**—Reconfigurable Intelligent Surfaces (RISs) have gained immense popularity in recent years because of their ability to improve wireless coverage and their flexibility to adapt to the changes in a wireless environment. These advantages are due to RISs' ability to control and manipulate radio frequency (RF) wave propagation. RISs may be deployed in inaccessible locations where it is difficult or expensive to connect to the power grid. Energy harvesting can enable the RIS to self-sustain its operations without relying on external power sources. In this paper, we consider the problem of energy harvesting for RISs in the absence of coordination with the ambient RF source. We consider both direct and indirect energy harvesting scenarios and show that the same mathematical model applies to them. We propose a sequential phase-alignment algorithm that maximizes the received power based on only power measurements. We prove the convergence of the proposed algorithm to the optimal value under specific circumstances. Our simulation results show that the proposed algorithm converges to the optimal solution in a few iterations and outperforms the random phase update method in terms of the number of required measurements.

**Index Terms**—Energy harvesting, reconfigurable intelligent surface, phased array, zero-energy devices.

## I. INTRODUCTION

Future wireless networks should provide seamless connectivity for the rapidly growing number of devices and services. If wireless networks are implemented in the same manner as before, the energy consumption would keep increasing dramatically with the traffic volume. From both carbon footprint and energy consumption perspectives, it is a necessity to develop energy-saving techniques that can be implemented in the network nodes including low-power and zero-energy devices [1]–[3].

Traditional wireless networks have no control over the radio propagation environment. Providing connectivity for regions with low signal-to-noise ratio (SNR) comes at cost of deploying more sophisticated transmission schemes, more radio resources such as antennas and spectrum and consequently consuming more energy [4], [5].

With the emergence of the reconfigurable intelligent surfaces (RISs), several limiting factors associated with the propagation environment can be eliminated. A RIS can manipulate the propagation environment to increase the signal strength in the desired direction and guide the electromagnetic waves toward the receiver via engineered reflections [6]–[10]. The

RIS is primarily envisioned for providing coverage for regions that are blocked by objects [5]. For instance, a RIS can be deployed in a city with dense buildings and poor line-of-sight (LoS) conditions, or it can also be deployed in homes, where the walls obstruct the signal path.

In the presence of a wired power supply, RIS may not have clear benefits compared to relays and small cells, and the respective advantages are debatable. However, if the RIS is self-sustainable, it opens up new possibilities for deployment with no competition. This is where energy harvesting comes into play. By harvesting energy from radio frequency (RF) signals that are already present in the environment, the RIS can operate without relying on external power sources [11]. This is particularly beneficial in situations where the RIS is deployed in remote or inaccessible locations where it can be difficult or expensive to provide a continuous power source. In [12], the authors developed a model for the RIS power consumption that is based on the number of elements and their phase resolution. Higher phase resolution in the RIS increases the complexity and the power consumption [13].

The study [14] considers a hybrid-relaying scheme empowered by a self-sustainable RIS to simultaneously improve the downlink energy transmission and uplink information transmission. The authors proposed time-switching and power-splitting schemes for RIS operation. The paper [15] proposes a novel framework for wireless power transfer (WPT) system using a RIS to improve power transfer efficiency. The proposed framework employs independent beamforming to replace conventional joint beamforming, which results in higher efficiency.

The state-of-the-art techniques consider perfect channel state information (CSI) at the RIS, which is obtained by coordination between the transmitters and the RIS. The existing solutions require extra hardware (i.e., multiple RF receiver to measure both amplitude and phase to obtain CSI) and signaling, which in turn increases the energy consumption and cost of the RIS.

In this paper, we consider a different scenario, where the RIS must configure itself without RF receivers. The proposed method makes power measurements in the energy harvesting units and uses them to maximize the harvesting power. The main contributions of this paper as compared to the existing works are as follows.

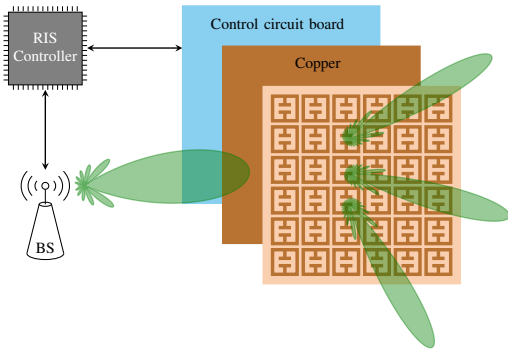


Fig. 1. Hardware structure of a RIS.

- We propose a sequential phase-alignment algorithm to maximize the received power at the harvesting unit based on power measurements.
- We prove the optimality of the proposed algorithm analytically.
- Our simulation results show that the proposed algorithm greatly outperforms the benchmark random phase-update method in terms of the number of required measurements to achieve the optimum.

The remainder of this paper is organized as follows. Section II describes the RIS hardware architecture, two different energy harvesting schemes in the RIS, and the phase alignment problem. Section III describes the proposed abstract model of the RIS operation and the proposed solution. Simulation results are presented in Section IV, while Section V provides our conclusions.

*Notations:* We denote sets by upper-case script letters, e.g.,  $\mathcal{S}$ . The only exceptions are the sets of natural numbers, real numbers, and complex numbers that we represent with  $\mathbb{N}$ ,  $\mathbb{R}$ , and  $\mathbb{C}$ , respectively. The cardinality of a set  $\mathcal{S}$  is represented by  $|\mathcal{S}|$ . Vectors are indicated by lower-case bold-face letters, e.g.,  $\mathbf{x}$ , and  $x_i$  denotes the  $i$ th element of  $\mathbf{x}$ . We represent matrices by upper-case bold-face letters, e.g.,  $\mathbf{A}$ . We also use  $\triangleq$  to indicate an equal by definition sign. With  $(\cdot)^T$ , we denote the transpose operator. We denote the imaginary unit by  $j \triangleq \sqrt{-1}$ . We represent the conjugate of a complex number  $z$  with  $z^*$ . However, we denote the optimal solution with the superscript  $\star$ , e.g.,  $x^\star$ . Also, the operation  $\text{Arg}(z)$  returns the single-valued argument of  $z$  that lies within the interval  $(-\pi, \pi]$ , while  $\arg(z)$  returns the set of all possible values of the argument of  $z$ .

## II. PROBLEM DESCRIPTION

This section presents 1) the RIS device architecture, 2) the energy harvesting schemes, and 3) the phase alignment problem for RIS-assisted energy harvesting.

### A. RIS Hardware Architecture

Fig. 1 illustrates the hardware architecture of a typical RIS. The front layer consists of several metal elements that

are printed on a dielectric substrate and arranged in a two-dimensional array to reflect the incoming signals. For each patch element, there is a controllable circuit that is used to adjust the phase of the reflected signals and direct the signal in a desired direction. There is a control circuit board that can control the reflection amplitudes and phase shifts of the patch elements. The RIS controller can communicate with the network components such as base stations (BSs) via a connectivity interface [5]. Finally, the RIS requires a power supply to adjust the phases and then maintain the desired reflection state.

### B. Energy Harvesting Schemes

In general, an RIS can harvest RF energy directly or indirectly from an ambient RF source. We will describe these scenarios below and later show that they lead to system models of the same kind.

1) *Direct Energy Harvesting:* The RIS elements are capable of reflecting and receiving the incident electromagnetic (EM) waves. During the harvesting phase, the RIS operates in the reception mode, where it combines the received signals from each element with some phase shifts.<sup>1</sup> The RIS can use the harvested energy to fully sustain its operation or, if the energy is insufficient, it can decrease the consumption from other energy sources, as a first step toward achieving a zero-energy RIS system. The abstract model of the direct energy harvesting operation is shown in Fig. 2a.

2) *Indirect Energy Harvesting:* The RIS is generally deployed and designed to reflect the EM waves towards a desired location (typically a receiver location). Inspired by this principle, the energy harvesting device can alternatively be deployed in front of the RIS (at a short distance) and the phases of the RIS elements can be aligned so they combine constructively at the location of the energy harvesting device. This device then can return the energy to the RIS via a cable. The concept of indirect energy harvesting is demonstrated in Fig. 2b.

### C. Phase Alignment Problem for the Energy Harvesting

We consider a scenario of energy harvesting (EH) from an ambient RF source by an RIS with no prior CSI, and there is no coordination between the RIS and the RF transmitter. We assume that the transmit power and the location of the transmitter are unknown.<sup>2</sup>

For the direct (indirect) scheme, we assume the measured RF power by the RIS (EH device) has the following expression [8]

$$y = \left| \sum_{n=1}^N z_n e^{j\vartheta_n} \right|^2, \quad (1)$$

<sup>1</sup>There is a type of metasurface implementation called holographic beam-forming that can pass the incident EM waves from one side to the other. The metamaterial can add adjustable phase shifts, similar to a phased array, but with a different implementation [16].

<sup>2</sup>This scenario is more practical (compared to a scenario with coordination between the transmitter and the RIS) as the transmitter may not be designed to coordinate the CSI with the RIS or only do it when it requests that the RIS is supporting its data transmissions.

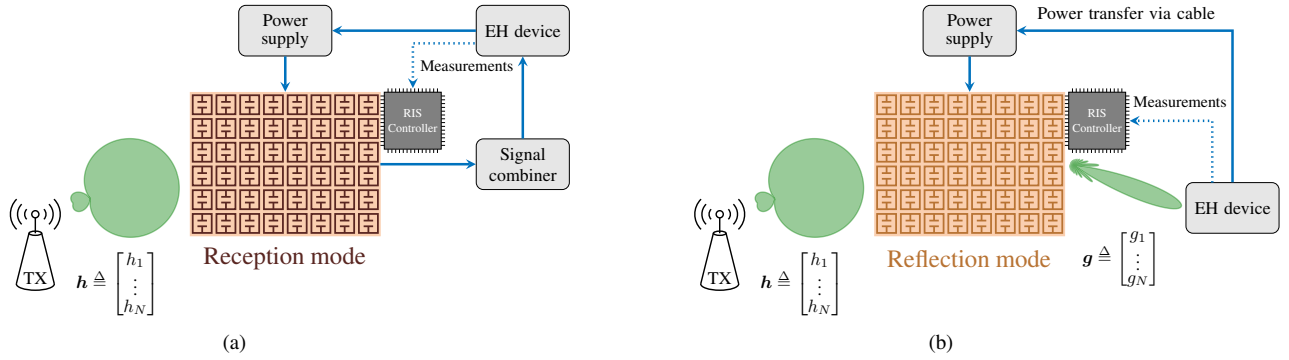


Fig. 2. Energy harvesting schemes: (a) direct (b) indirect.

where  $z_n \in \mathbb{C}$  for each  $0 \leq n \leq N$ . In (1),  $z_n$  not only includes all channel gains between transmitters and the energy harvester (except the adjustable phase shift  $\vartheta_n$ ), but also takes into account the transmission power. Also,  $\vartheta_n \in [0, 2\pi)$  is the adjustable phase shift of the  $n$ th element of the RIS. Also  $y$  represents the measured received power that is obtained from the reading of the power in the EH device [8], [17].<sup>3</sup>

For direct and indirect energy harvesting schemes, and for all  $1 \leq n \leq N$ , we have

$$z_n \triangleq \begin{cases} P_t h_n, & \text{Direct EH} \\ P_t h_n g_n, & \text{Indirect EH,} \end{cases} \quad (2)$$

where  $h_n \in \mathbb{C}$  and  $g_n \in \mathbb{C}$  are the channel gains from the transmitter to the RIS element  $n$  and from the RIS element  $n$  to the EH device in the indirect case, respectively. Also,  $P_t$  is the transmit power.

We assume no CSI is available at the RIS controller (i.e.,  $z_n$  is unavailable to the RIS). This scenario is more general compared to a scenario with coordination between the transmitters and the RIS, since the transmitter might lack a protocol to reach the RIS and can even be unaware of its existence.

The values of  $\{z_n\}_{n=1}^N$  depend on the geometry and propagation environment and can be estimated by measuring amplitude and phase using RF receiver circuits. Since the RIS lack such RF chains, the RIS cannot estimate the amplitudes and phases. Hence, the values of  $\{z_n\}_{n=1}^N$  will remain unknown to the RIS. On the other hand, with power measurement at the EH device, the RIS can measure the combined power from all elements for any feasible phase configuration.

The general optimization problem is to maximize the received RF power<sup>4</sup> by finding proper phase shifts (i.e.,  $\vartheta \triangleq [\vartheta_1, \dots, \vartheta_N]^T$ ) for the RIS array.

<sup>3</sup>Power measurements can be obtained from the input of the energy harvesting unit using a circuit such as a voltmeter. Alternatively, power measurements can be applied at the output of the energy harvesting unit by compensating for the nonlinear harvesting conversion efficiency.

<sup>4</sup>Note that the harvested RF power is a nonlinear function of the received RF power that is called the conversion efficiency function. We consider the problem of choosing optimal phase shift  $\vartheta^*$  for the RIS elements to maximize the harvesting RF power. However, since the conversion efficiency function is generally an increasing function, the optimal solution for maximization of the harvesting RF power is equivalent to the one for the maximization of the measured received RF power.

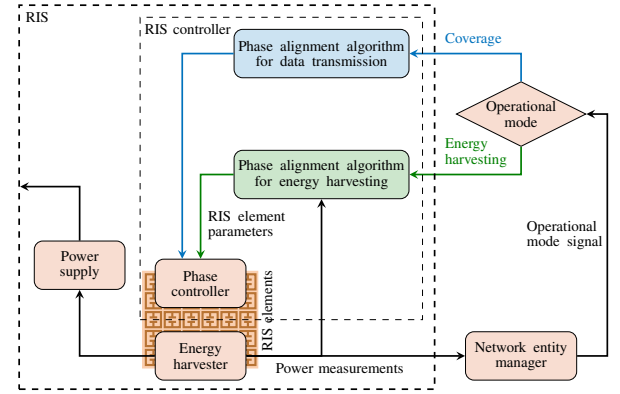


Fig. 3. The abstract model of the operation of a RIS with an energy harvesting module.

### III. PROPOSED PHASE ALIGNMENT SCHEME

In this section, we investigate the problem of received RF power maximization using a dynamic sequence of power measurements. We propose a model for the RIS energy harvesting operations and an algorithm to find the optimal phase of RIS elements.

#### A. An Abstract Model of the Proposed RIS Operation

A simplified model of the operation of an RIS with an energy harvesting module is shown in Fig. 3. The network entity manager can assess the network environment, including but not limited to network demand, SNR, and power measurements from the RIS, and determine if the RIS should function to provide connectivity or to harvest energy. Within the RIS controller, the preferred phase of each element can be determined based on functionality, and the controller can adjust the phase of the elements accordingly. The energy harvester can be located either outside or inside the RIS surface. It sends power measurements to a phase alignment algorithm implemented in the network entity manager module. These values can be used by the network entity manager to decide whether the RIS should be in energy harvesting or data transmission mode. After reaching an appropriate phase configuration, the harvested energy can be fed back to the power supply to be used by the RIS.

## B. Proposed Algorithm

We consider an ideal scheme, where the RIS is capable of adding continuous phase shifts to the incident EM waves. First, we start with stating Lemma 1 that provides a mechanism to find the optimal phase shifts in the case of known CSI, then based on that, we develop our proposed algorithm that require no a priori CSI.

*Lemma 1:* Let  $f : \mathbb{R}^N \rightarrow \mathbb{R}$  be the function

$$f(\boldsymbol{\vartheta}) \triangleq \left| \sum_{n=1}^N z_n e^{j\vartheta_n} \right|^2, \quad (3)$$

where  $z_n \in \mathbb{C}$  for all  $1 \leq n \leq N$ . The optimal variable  $\boldsymbol{\vartheta}^* \triangleq (\vartheta_1^*, \dots, \vartheta_N^*)$  that maximizes  $f(\cdot)$  is given by

$$\vartheta_n^* = \vartheta_0 - \arg(z_n), \quad (4)$$

where  $\vartheta_0 \in \mathbb{R}$ , and

$$f(\boldsymbol{\vartheta}^*) = \left( \sum_{n=1}^N |z_n| \right)^2 \quad (5)$$

is the maximum value of  $f(\cdot)$ .

*Theorem 2:* Let  $f : \mathbb{R} \rightarrow \mathbb{R}$  be a function of the form

$$f(\vartheta) = |z_0 + z e^{j\vartheta}|^2,$$

where  $z_0, z \in \mathbb{C}$ . Without knowing the explicit values of  $z_0$  and  $z$ , the optimal variable  $\vartheta^*$  that maximizes  $f(\cdot)$  can be computed as

$$\vartheta^* = \arg(x_2 + jx_3), \quad (6)$$

where  $\mathbf{x} \triangleq \mathbf{A}^{-1} \mathbf{y}$ . The matrix  $\mathbf{A}$  is defined as

$$\mathbf{A} \triangleq \begin{bmatrix} 1 & \cos(\varphi_1) & \sin(\varphi_1) \\ 1 & \cos(\varphi_2) & \sin(\varphi_2) \\ 1 & \cos(\varphi_3) & \sin(\varphi_3) \end{bmatrix}, \quad (7)$$

and  $\mathbf{y} \triangleq [f(\varphi_1), f(\varphi_2), f(\varphi_3)]^T$  is the measurement vector. Note that  $\varphi_1, \varphi_2, \varphi_3 \in [0, 2\pi)$  are selected such that  $\det(\mathbf{A}) \neq 0$ .

*Proof.* The proof is provided in Appendix A.

In general, Theorem 2 allows for the computation of the optimal phase shift using only three measurements, without requiring knowledge of the explicit expression of the function. Specifically, for the measurement phases  $\varphi_1 = 0$ ,  $\varphi_2 = \pi/2$ , and  $\varphi_3 = \pi$ , a simple expression for the optimal phase shift can be obtained as follows:

$$\vartheta^* = \arg(y_1 - y_3 + j(2y_2 - y_1 - y_3)). \quad (8)$$

Algorithm 1 is a sequential, iterative phase update algorithm. At each iteration, adjusting the phase of each element requires measuring the received power for three different phase configurations. The algorithm updates the phase of one element using (8), then proceeds to the next element until all  $N$  elements have had their phases updated. This process is repeated  $M$  times.

Figure 4 presents a toy example that demonstrates the different steps of the proposed algorithm. The vector representation

---

**Algorithm 1:** The proposed phase-alignment algorithm for power maximization

---

**Input:** The number of RIS elements  $N$  and the number of iterations  $M$

**Output:** Near-optimal phase vector  $\boldsymbol{\vartheta}^*$  that maximizes the received power.

**Initialize:**  $\boldsymbol{\vartheta} \leftarrow \boldsymbol{\vartheta}_0$ ,  $m \leftarrow 0$ , and  $\mathbf{e}_n$  is a vector, where the component  $n$  is 1 and all other components are 0.

**while**  $m < M$  **do**

$m \leftarrow m + 1$ ;

$n \leftarrow 1$ ;

**while**  $n \leq N$  **do**

$y_1 \leftarrow$  the measured power for the phase configuration  $\boldsymbol{\vartheta}$ ;

$y_2 \leftarrow$  the measured power for the phase configuration  $\boldsymbol{\vartheta} + \frac{\pi}{2} \mathbf{e}_n$ ;

$y_3 \leftarrow$  the measured power for the phase configuration  $\boldsymbol{\vartheta} + \pi \mathbf{e}_n$ ;

$\boldsymbol{\vartheta} \leftarrow \boldsymbol{\vartheta} + \arg(y_1 - y_3 + j(2y_2 - y_1 - y_3)) \mathbf{e}_n$ ;

$n \leftarrow n + 1$ ;

**end**

**end**

$\boldsymbol{\vartheta}^* \leftarrow \boldsymbol{\vartheta}$ ;

---

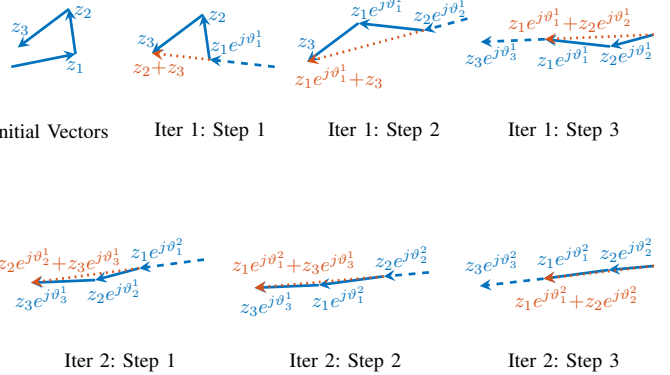


Fig. 4. Visualization of the proposed algorithm in different steps for a toy example with  $N = 3$ .

shows that initially, the vectors are misaligned, leading to a relatively small amplitude of their sum compared to a scenario where they are aligned in the same direction. The algorithm updates the phase of each vector to match with the sum of the others. As the algorithm progresses and reaches the end of the second iteration, the vectors become almost aligned in the same direction, resulting in a nearly maximum amplitude of their sum.

*Theorem 3:* The proposed Algorithm 1 converges to the maximum value of the function  $f(\boldsymbol{\vartheta}) = \left| \sum_{n=1}^N z_n e^{j\vartheta_n} \right|^2$  as  $M \rightarrow \infty$ .

*Proof.* The proof is provided in Appendix B.



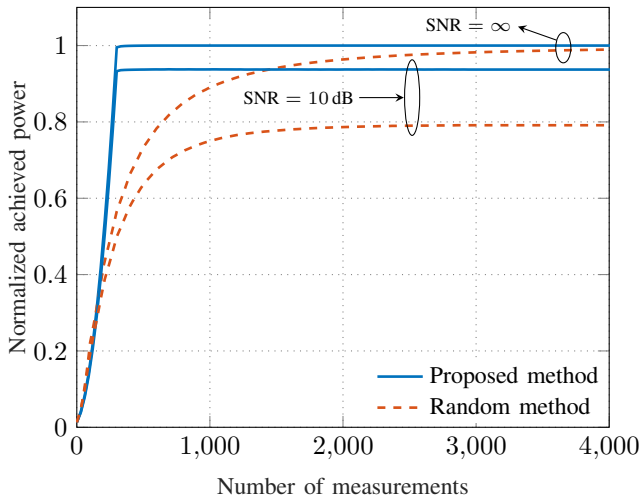


Fig. 5. Normalized achieved power versus the number of measurements for the proposed and random methods.

### C. A Random Algorithm

We use a random algorithm as a benchmark for the proposed algorithm. The basic concept is that, at each step, the algorithm picks a single element of the RIS sequentially and assigns a random phase value from a uniform distribution over the interval  $[0, 2\pi)$ . The new power measurement is then compared to the previous one. If the power increases, the algorithm updates the phase and moves on to the next element. If the measured power decreases, the algorithm maintains the previous phase and proceeds to the next element.

## IV. PERFORMANCE EVALUATION

In this section, we evaluate the performance of our proposed algorithm and compare it to the random phase update method. We use a RIS with 100 elements and generate random complex Gaussian distributed values with unit variance for  $\{z_n\}_{n=1}^N$ . We conducted Monte-Carlo simulations and compared the results with those obtained from the random phase update method.

Fig. 5 illustrates the normalized achieved power versus the number of power measurements for the proposed and random methods. The proposed method uses three measurements per phase update of each element and converges to its final value after 300 measurements (i.e.,  $3N$ ), while the random one requires ten times more measurements as it has a slow convergence rate. Even in the presence of the noise, at the SNR of 10 dB the proposed algorithm reaches the 93% of the maximum achievable power [18].

Fig. 6 shows the cumulative distribution function (CDF) of the relative achieved power for both the proposed and random algorithms, compared to the optimum. We conducted 1000 simulations with randomly generated channels. The results indicate that the proposed algorithm after the first iteration performs significantly better than the random one after ten iterations. Although the proposed algorithm still performs

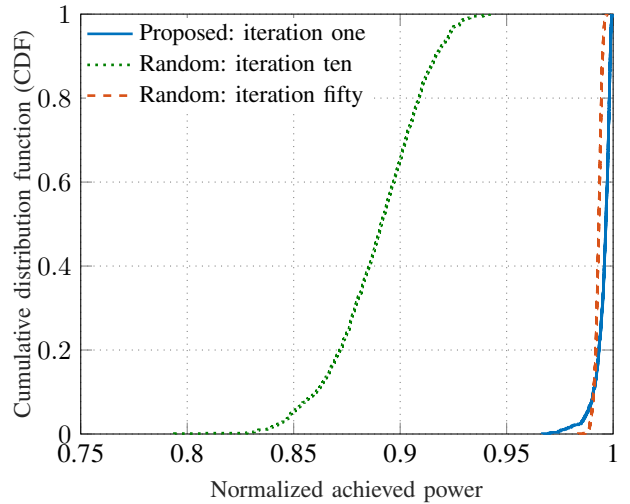


Fig. 6. The CDF of the normalized achieved power for the proposed and random algorithms.

slightly better than the random one after fifty iterations, the latter appears to be slightly more stable.

## V. CONCLUSIONS

This paper has presented a method for energy harvesting at a RIS from an ambient RF source in the absence of coordination with the source. The objective was to maximize the received power by adjusting the phases of the RIS elements based only on power measurements, obtained without having a RF receiver. The proposed sequential algorithm is proved to converge to the optimum and outperformed the random phase update method in terms of convergence rate. In future work, we will extend this study to more general scenarios, including the case with discrete phase shifts.

### APPENDIX A PROOF OF THEOREM 2

Let us define

$$\mathbf{x} \triangleq [ |z_0|^2 + |z|^2, 2 \operatorname{Re}(z_0 z^*), 2 \operatorname{Im}(z_0 z^*) ]^T. \quad (9)$$

From Lemma 1 and (9), we have

$$\begin{aligned} \vartheta^* &= \arg(z_0) - \arg(z) \\ &= \arg(z_0 z^*) \\ &= \arg(\operatorname{Re}(z_0 z^*) + j \operatorname{Im}(z_0 z^*)) \\ &= \arg(x_2 + j x_3). \end{aligned}$$

Therefore, we can compute the optimal phase shift from  $\mathbf{x}$ . We show that one can compute  $\mathbf{x}$  using the received power from three different measurements. By expanding the function  $f(\varphi_l)$ , we get

$$\begin{aligned} f(\varphi_l) &= |z_0|^2 + |z|^2 + 2 \operatorname{Re}(z_0 z^*) \cos(\varphi_l) + 2 \operatorname{Im}(z_0 z^*) \sin(\varphi_l) \\ &= \mathbf{a}_l^T \mathbf{x}, \end{aligned} \quad (10)$$

where  $\mathbf{a}_l \triangleq [1, \cos(\varphi_l), \sin(\varphi_l)]^T$ , for  $1 \leq l \leq 3$ .

Assuming  $\mathbf{A} \triangleq [\mathbf{a}_1, \mathbf{a}_2, \mathbf{a}_3]^\top$ , and  $\mathbf{y} = [f(\varphi_1), f(\varphi_2), f(\varphi_3)]^\top$ , we have  $\mathbf{Ax} = \mathbf{y}$ , or  $\mathbf{x} = \mathbf{A}^{-1}\mathbf{y}$  for  $\det(\mathbf{A}) \neq 0$ .

## APPENDIX B PROOF OF THEOREM 3

We denote the phase-shift vector generated by the algorithm at iteration  $m$  up to the element  $n$  with  $\boldsymbol{\vartheta}^k$ , where  $k = mN + n$ . We prove that for a given  $N$ ,  $\lim_{k \rightarrow \infty} f(\boldsymbol{\vartheta}^k) = \max_{\boldsymbol{\vartheta}} f(\boldsymbol{\vartheta})$ . For any integer  $1 \leq n \leq N$  and an integer  $k \geq 1$ , we define

$$w_n^k \triangleq \sum_{\substack{i=1 \\ i \neq n}}^N z_i e^{j\vartheta_i^k}. \quad (11)$$

Hence, we have  $f(\boldsymbol{\vartheta}^k) = |w_n^k + z_n e^{j\vartheta_n^k}|^2$ . At the phase update  $k + 1$ , the algorithm only updates the phase of the element  $n$  ( $w_n^{k+1} = w_n^k$ ) as  $f(\boldsymbol{\vartheta}^{k+1}) = |w_n^k + z_n e^{j\vartheta_n^{k+1}}|^2$ . According to the Theorem 2, we have

$$f(\boldsymbol{\vartheta}^{k+1}) = |w_n^k + z_n e^{j\vartheta_n^{k+1}}|^2 \geq |w_n^k + z_n e^{j\vartheta_n^k}|^2 = f(\boldsymbol{\vartheta}^k). \quad (12)$$

Therefore,  $f(\boldsymbol{\vartheta}^1), f(\boldsymbol{\vartheta}^2), \dots$  form an increasing sequence. Moreover, according to the Lemma 1, the set  $\mathcal{F} \triangleq \{f(\boldsymbol{\vartheta}^k); k \in \mathbb{N}\}$  is upper bounded by  $(\sum_{n=1}^N |z_n|)^2$ . Therefore, according to the monotone convergence theorem, we have

$$\lim_{k \rightarrow \infty} f(\boldsymbol{\vartheta}^k) = \sup \mathcal{F} \leq \left( \sum_{n=1}^N |z_n| \right)^2. \quad (13)$$

If we show that  $\sup \mathcal{F} = (\sum_{n=1}^N |z_n|)^2$ , the proof is complete. Let's define  $\boldsymbol{\vartheta}^* \triangleq \lim_{k \rightarrow \infty} \boldsymbol{\vartheta}^k$ . For the phase shift vector  $\boldsymbol{\vartheta}^*$ , any further phase update will not increase  $f(\cdot)$ . In other words, for updating element  $n$ , we should apply Theorem 2 to the following function

$$f(\boldsymbol{\vartheta}^*) = |w_n^* + z_n e^{j\vartheta_n^*}|^2, \quad (14)$$

where  $w_n^* \triangleq \sum_{\substack{i=1 \\ i \neq n}}^N z_i e^{j\vartheta_i^*}$ . Since any further update will not increase the value of  $f(\cdot)$ , therefore for all  $1 \leq n \leq N$ , we have  $\text{Arg}(z_n e^{j\vartheta_n^*}) = \text{Arg}(w_n^*)$ . Using Lemma 4, we have

$$\text{Arg}(z_1 e^{j\vartheta_1^*}) = \text{Arg}(z_2 e^{j\vartheta_2^*}) = \dots = \text{Arg}(z_N e^{j\vartheta_N^*}), \quad (15)$$

or

$$\text{Arg}(z_1) + \vartheta_1^* = \dots = \text{Arg}(z_N) + \vartheta_N^* = \vartheta_0 \pmod{2\pi}. \quad (16)$$

Therefore, we have  $\vartheta_n^* = \vartheta_0 - \arg(z_n)$ , for all  $1 \leq n \leq N$ , that are according to the Lemma 1, the phase shifts that maximize  $f(\cdot)$ .

*Lemma 4:* Assume for each  $1 \leq n \leq N$ ,  $u_n \triangleq \sum_{\substack{i=1 \\ i \neq n}}^N z_i$ , if  $\text{Arg}(z_n) = \text{Arg}(u_n)$  for all  $1 \leq n \leq N$ , then  $\text{Arg}(z_1) = \text{Arg}(z_2) = \dots = \text{Arg}(z_N)$ .

*Proof.* For  $1 \leq m, n \leq N$  and  $m \neq n$ , we have  $\text{Arg}(z_m) = \text{Arg}(u_m)$  and  $\text{Arg}(z_n) = \text{Arg}(u_n)$ , therefore, for some real positive  $c_m$  and  $c_n$ , we have  $z_m = c_m u_m$  and  $z_n = c_n u_n$ . Assuming  $u_{m,n} \triangleq \sum_{\substack{i=1 \\ i \neq m,n}}^N z_i$ , we have

$$z_m = c_m (z_n + u_{m,n}) \quad (17)$$

$$z_n = c_n (z_m + u_{m,n}). \quad (18)$$

After some algebraic manipulations, we obtain

$$z_m = \frac{c_m (1 + c_n)}{c_n (1 + c_m)} z_n. \quad (19)$$

Hence,  $\text{Arg}(z_m) = \text{Arg}(z_n)$  and the proof is complete.

## REFERENCES

- [1] M. Tavana, M. Ozger *et al.*, "Wireless power transfer for aircraft IoT applications: System design and measurements," *IEEE Internet Things J.*, vol. 8, no. 15, pp. 11 834–11 846, 2021.
- [2] M. Tavana, E. Björnson, and J. Zander, "Range limits of energy harvesting from a base station for battery-less Internet-of-things devices," in *IEEE International Conference on Communications (ICC)*, 2022.
- [3] M. Tavana, E. Björnson, and J. Zander, "Multi-site energy harvesting for battery-less internet-of-things devices: Prospects and limits," in *IEEE 96th Vehicular Technology Conference (VTC2022-Fall)*, 2022, pp. 1–6.
- [4] A. Goldsmith, *Wireless Communications*. Cambridge University Press, 2005.
- [5] M. Di Renzo, A. Zappone *et al.*, "Smart radio environments empowered by reconfigurable intelligent surfaces: How it works, state of research, and the road ahead," *IEEE J. Sel. Areas Commun.*, vol. 38, no. 11, pp. 2450–2525, 2020.
- [6] W. Tang, M. Z. Chen *et al.*, "Wireless communications with programmable metasurface: New paradigms, opportunities, and challenges on transceiver design," *IEEE Wireless Communications*, vol. 27, no. 2, pp. 180–187, 2020.
- [7] L. Subrt and P. Pechac, "Controlling propagation environments using intelligent walls," in *European Conference on Antennas and Propagation (EUCAP)*, 2012, pp. 1–5.
- [8] E. Björnson, H. Wymeersch *et al.*, "Reconfigurable intelligent surfaces: A signal processing perspective with wireless applications," *IEEE Signal Processing Mag.*, vol. 39, no. 2, pp. 135–158, 2022.
- [9] W. Tang, M. Z. Chen *et al.*, "Wireless communications with reconfigurable intelligent surface: Path loss modeling and experimental measurement," *IEEE Trans. Wireless Commun.*, vol. 20, no. 1, pp. 421–439, 2021.
- [10] Q. Wu, S. Zhang *et al.*, "Intelligent reflecting surface-aided wireless communications: A tutorial," *IEEE Trans. Commun.*, vol. 69, no. 5, pp. 3313–3351, 2021.
- [11] K. Ntontin, A. A. Boulogeorgos *et al.*, "Wireless energy harvesting for autonomous reconfigurable intelligent surfaces," *IEEE Trans. Green Commun. Netw.*, vol. 7, no. 1, pp. 114–129, 2023.
- [12] C. Huang, A. Zappone *et al.*, "Reconfigurable intelligent surfaces for energy efficiency in wireless communication," *IEEE Trans. Wireless Commun.*, vol. 18, no. 8, pp. 4157–4170, 2019.
- [13] R. Méndez-Rial, C. Rusu *et al.*, "Hybrid MIMO architectures for millimeter wave communications: Phase shifters or switches?" *IEEE Access*, vol. 4, pp. 247–267, 2016.
- [14] B. Lyu, P. Ramezani *et al.*, "Optimized energy and information relaying in self-sustainable IRS-empowered WPCN," *IEEE Trans. Commun.*, vol. 69, no. 1, pp. 619–633, 2021.
- [15] Y. Cheng, W. Peng, and T. Jiang, "Self-sustainable RIS aided wireless power transfer scheme," *IEEE Trans. Veh. Technol.*, vol. 72, no. 1, pp. 881–892, 2023.
- [16] E. J. Black, "Holographic beam forming and MIMO," Pivotal Commware, Tech. Rep., 2017.
- [17] S. Haykin, *Communication Systems*. John Wiley & Sons, 2008.
- [18] M. Tavana, M. Masoudi, and E. Björnson, "Energy harvesting maximization for reconfigurable intelligent surfaces using amplitude measurements," *Submitted to IEEE Trans. Commun.*, 2023.